Clin Transl Imaging (2017) 5:507–523
https://doi.org/10.1007/s40336-017-0251-x

EXPERT REVIEW

PET probes for imaging pancreatic islet cells

Chang-Tong Yang[1] · Krishna K. Ghosh[1] · Parasuraman Padmanabhan[1] · Oliver Langer[3,4,5] · Jiang Liu[6] · Christer Halldin[1,2] · Balázs Z. Gulyás[1,2]

Received: 6 July 2017 / Accepted: 18 September 2017 / Published online: 3 October 2017

Abstract
Purpose PET can detect very low concentrations of the probes at subpicomolar range in the target tissue with high sensitivity. The development of PET probes for imaging pancreatic islet cells depends on several key elements: the amount of target receptors in the beta cells; the target specificity and the target tissue delivery. This review summarized the latest developments of PET probes which are targeting proteins including GLP-1, VMAT2, GPR44, antigen, glucokinase and reporter genes in the beta cell for imaging pancreatic islet cells.
Methods A survey of the literature was performed to select the articles focusing on the development of PET probes for proteins targeting in the beta cell. Since PET probe development for imaging pancreatic islet cells is a narrow research field, the literature survey comprised of those articles published from 1993 when first probe C-11 DTBZ was synthesized to 2017 in English journals. In-111 SPECT probes are included for comparison study.
Results A selection of 97 papers were identified following the literature review. The probes covered tritium-3-, carbon-11-, fluorine-18-, gallium-68-, copper-64- and indium-111 (for SPECT)-labeled radioligands. The PET imaging studies with the probes have been evaluated for in vitro, ex vivo, preclinical and clinical applications. Some issues of targeting probes have been addressed to develop ideal non-invasive PET probes for imaging pancreatic islet cells. From the literature, a number of new probes have been developed in recent years to improve their biological profile such as higher specific binding to target with lower nonspecific binding to surrounding tissue, or optimal residence time in the subjects.
Conclusion PET imaging modality for imaging pancreatic islet cell especially beta cell provided high resolution, high sensitivity, and accurate quantification through the biodistribution, pharmacokinetics and target binding of tracers. The demand for new PET probes for preclinical and clinical investigations is increasing. This review gives comprehensive overview of noteworthy probes which are proteins targeting in beta cell. The review provides some future research directions for this emerging field.

Keywords Positron emission tomography · Pancreatic islet cells · Diabetes · Imaging probes · Radiochemistry

✉ Chang-Tong Yang
yangct@ntu.edu.sg

1 Lee Kong Chian School of Medicine, Nanyang Technological University, 59 Nanyang Drive, Singapore 636921, Singapore

2 Department of Clinical Neuroscience, Karolinska Institutet, 171 76 Stockholm, Sweden

3 Department of Clinical Pharmacology, Medical University of Vienna, 1090 Vienna, Austria

4 Department of Biomedical Imaging and Image-Guided Therapy, Medical University of Vienna, 1090 Vienna, Austria

5 Center for Health and Bioresources, Biomedical Systems, AIT Austrian Institute of Technology GmbH, Seibersdorf, Austria

6 Cixi Institute of Biomedical Engineering, Ningbo Institute of Industrial Technology and Ningbo Institute of Materials Technology and Engineering, Chinese Academy of Sciences, Ningbo 315201, People's Republic of China

Introduction

The pancreas mainly consists of two types of tissues: endocrine and exocrine. The endocrine tissue which constitutes

only 1–2% of pancreatic mass is scattered heterogeneously in islets of Langerhans. Islets are comprised of four cell types: alpha, beta, delta and pancreatic polypeptide (PP)-cells in which beta cells (β-cells) are most abundant and constitute approximately 50–80% of the islets [1–4]. Insulin secreted by β-cell to adjust high blood glucose levels, and loss or destruction of beta cells causes diabetes. Diabetes mellitus (DM), a metabolic disorder which is characterized by high mortality hyperglycemia worldwide [5]. Two types of diabetes are distinguished based on different pathogenesis: Type 1 (T1D) or insulin dependent and Type 2 (T2D) or insulin resistant. Beta cell mass (BCM), which refer to as the collective β-cell numbers reduced significantly in both Type 1 and 2 diabetes patients compared to non-diabetic individuals. In T1DM, an autoimmune attack against pancreatic β-cells leads to a rapid loss of endocrine BCM; in T2DM, insulin resistance and β-cell dysfunction cause a progressive reduction of BCM ranging from 25 to 65% [6–9].

Functional loss of BCM is associated with both T1DM and T2DM. The information of human BCM during the progress of diabetes mellitus is mainly obtained from postmortem pancreatic biopsy studies. In vivo biopsies of the pancreas for determination of BCM in either healthy human or diabetic patients are unacceptable in clinical studies [10]. On the other hand, plasma measurements of β-cell function are not associated with the actual BCM [11]. Therefore, there is a need to develop non-invasive imaging techniques for effectively evaluating pancreatic β-cells and early diagnosis of metabolic diseases such as T1DM and T2DM which are β-cell related. Currently a variety of imaging modalities such as MRI [12–14], bioluminescence imaging [15, 16] and nuclear imaging have been used to investigate β-cell diseases. PET is standing out to provide high resolution, high sensitivity, and accurate quantification by effective methodologies.

Overall, low abundance of β-cells in the pancreas imposes challenges to BCM imaging. PET can detect very low concentrations of the tracers at subpicomolar range in the target tissue with high sensitivity [17]. PET probes have been applied for direct measurement of BCM depending on several key elements such as the amount of target receptors in the β-cells, its target specificity and the target tissue delivery [18]. The advanced sensitivity and imaging technologies are also the approaches to achieve this goal [19–21]. To noninvasively image pancreatic BCM, probes should be able to bind specifically to pancreatic β-cells. Probes targeting the proteins in β-cell include glucagon-like peptide 1 (GLP-1R), Type 2 vesicular monoamine transporters (VMAT2), G-protein-coupled receptor 44 (GPR44), antigen, glucokinase (GK), reporter genes, etc. [22–24]. This review summarized the recent developments of PET imaging probes for pancreatic islet cells especially β-cells, it provides comprehensive overview of probes targeting proteins in β-cell including H-3-, C-11-, F-18-, Ga-68-, Cu-64- and In-111 (for SPECT)-labeled radioligands (Table 1). The PET imaging studies with the probes cover in vitro, ex vivo, preclinical and clinical investigations. Nevertheless, the ideal PET probes for imaging pancreatic β-cells are yet to be developed.

GLP1-targeting probes

Glucagon-like peptide 1 (GLP-1) is a potent glucose-dependent insulin-tropic hormone, an endogenous incretin peptide which respond to nutrient ingestion to magnify insulin secreted from pancreatic β-cells by binding to the GLP-1 receptor [25]. Since GLP-1 is expressed highly on β-cells in the islets of Langerhans, it would be good for imaging pancreatic β-cell [26]. The GLP-1R is also important in glucose homeostasis as it is highly overexpressed in human insulinomas tumors derived from pancreatic β-cells [27]. Exendin-3 is a stable agonist of GLP-1R. Both ^{123}I-labeled GLP-1 and exendin-3 accumulated in rat insulinomas cell line RINm5F and can be potentially used for scintigraphic detection of insulinomas [28]. [Lys^{40}(DOTA)]-exendin-3 (Fig. 1) was labeled with ^{68}Ga to investigate the targeting of insulinomas using in vitro insulinoma tumor cells (INS-1) by PET/CT with [Lys^{40}(^{111}In-DTPA)]-exendin-3 as a reference for comparison [29]. After [Lys^{40}(^{68}Ga-DOTA)]-exendin-3 was injected, subcutaneous INS-1 tumors at the hind limb of BALB/c nude mice can be visualized clearly on PET/CT images.

Exendin-4, a subcutaneously administered peptide drug has been used for treatment of T2D. It is the one of the incretin mimetics that exhibited strong glucoregulatory activity. Exendin-4 isolated from heloderma suspectum venom has a structural relationship and closely related properties to GLP-1. Exendin-4 is an exendin-3 analogue, but different from exendin-3, in which two amino acid substitutions are involved in internalization of receptor–ligand complex, Gly^2–Glu^3 in place of Ser^2–Asp^3. The structural differences lead to exendin-4 distinct from exendin-3 in its bioactivity. Since then, a series of exendin-4-based radiopharmaceuticals as PET/CT and SPECT/CT probes were developed for GLP-1R targeting [30–33]. ^{111}In-labeled [Lys^{40}(Ahx-DTPA)NH$_2$]exendin-4 (Ahx = 6-aminohexanoic acid), [Lys^{40}(Ahx-DOTA)NH$_2$]exendin-4, ^{99m}Tc-labeled [Lys^{40}(Ahx-HYNIC/EDDA)NH$_2$]exendin-4 (HYNIC = hydrazinonicotinamide, EDDA = ethylenediaminediacetic acid) and ^{68}Ga-labeled [Lys^{40}(Ahx-DOTA)NH$_2$]exendin-4 demonstrated the promising pharmacokinetics, respectively. The imaging data showed they are suitable candidates for GLP-1R-targeting studies. The high specific uptake of [Lys^{40}(Ahx-DTPA-^{111}In)NH$_2$] exendin-4 in the Rip1Tag2 tumor which is the tumor of the pancreatic β-cells with highly reproducible multistage

Table 1 Representative PET probes for imaging of pancreatic islet cells

Probe targets	Probe name	Application	References
GLP-1	[Lys^{40}(^{68}Ga-DOTA)]exendin-3	In vitro, preclinical	[29]
	[Lys^{40}(Ahx-DTPA-^{111}In)NH_2] exendin-4	Preclinical, clinical	[30, 31]
	[Lys^{40}(Ahx-DOTA-^{68}Ga)NH_2] exendin-4	Preclinical, clinical	[32, 33]
	^{18}F-FREM-EM3106B	Preclinical	[34]
	^{18}F-FBEM-Cys^{40}-exendin-4	Preclinical	[35]
	^{18}F-AIF-NOTA	Preclinical	[36]
	^{18}F-FBA-exendin(9-39)	Preclinical	[37]
	^{18}F-TTCO-Cys^{40}-Exendin-4	Preclinical	[38]
	^{64}Cu-DO3A-VS-Cys^{40}-exendin-4	Preclinical	[39, 40]
	^{64}Cu-Lys^{40}-DOTA-NH_2-exendin-4	Ex vivo	[41]
	^{64}Cu-NODAGA-exendin-4	Preclinical	[42]
	^{68}Ga-DO3A-VS-Cys^{40}-exendin-4	Preclinical, clinical	[43–45, 51]
	^{68}Ga-NOTA-exendin-4	Clinical	[49, 50]
VMAT2	^{11}C-(+)-DTBZ	Preclinical, clinical	[59–67]
	^{18}F-fluoroepoxide-DTBZ	Preclinical	[68]
	^{18}F-FP-(+)-DTBZ	Preclinical, clinical	[69–73]
	^{18}F-FE-(+)-DTBZ	Preclinical	[74, 75]
	^{18}F-FE-DTBZ-d4	In vitro, preclinical	[76]
	^{64}Cu-CB-TE2A-(+)-DTBZ	Ex vivo	[77]
GPR44	^{3}H-AZD3825	In vitro, preclinical	[79]
	^{11}C/^{3}H-AZ Compound X	In vitro	[80]
Antigen	^{111}In-DTPA-IC2	Preclinical	[82]
	^{125}I-γ-G	In vitro	[83]
Glucokinase	^{11}C-AZ12504948	Preclinical	[84]
Reporter genes	^{18}F-FHBG	In vitro, ex vivo	[86–89]

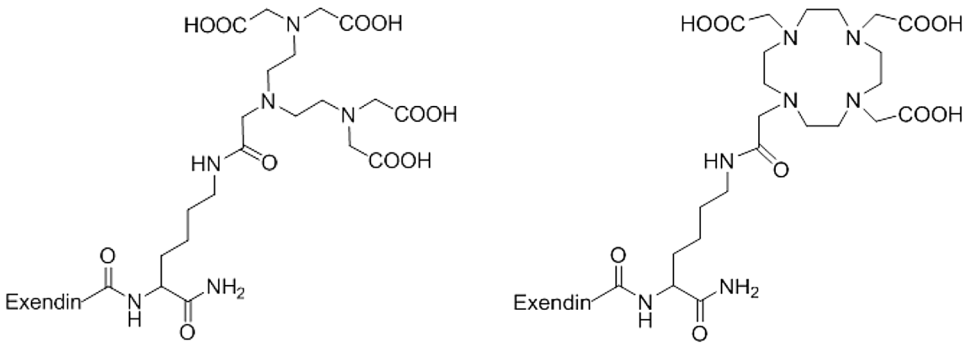

Fig. 1 Schematic structures of [Lys^{40}(DTPA)]-exendin-3 and [Lys^{40}(DOTA)]-exendin-3 (Ref. [29])

tumor progression lead to successful imaging of small insulinomas in this tumor mouse model [30]. The first clinical study of [Lys^{40}(Ahx-DTPA-^{111}In)NH_2]exendin-4 with GLP-1R imaging performing on two patients with insulinomas was successful [31]. The insulinomas in these two patients were either not localized or unsatisfactorily localized by other conventional imaging methods. It indicated that GLP-1R scanning could offer a new diagnostic approach to localize the small insulinomas in human. Ga^{68}-labeled [Lys^{40}(Ahx-DOTA-^{68}Ga)NH_2]exendin-4 displayed similar biodistributions and pharmacokinetics in human as its in^{111}-labeled analogue [32]. PET/CT study with [Lys^{40}(Ahx-DOTA-^{68}Ga)NH_2]exendin-4 showed that high specific uptake in the insulinoma tumor with a high tumor-to-background ratio. [Lys^{40}(Ahx-DOTA-^{68}Ga)NH_2] exendin-4 PET/CT was able to localize the hidden insulinomas with highly efficient detection [33].

Novel GLP-1 analogue EM3106B was conjugated with *N*-2-(4-^{18}F-fluorobenzamido)-ethylmaleimide, ^{18}F-labeled through a maleimide-based prosthetic group ^{18}F-FREM, forming the first ^{18}F-labeled GLP-1 PET probe ^{18}F-FREM-EM3106B for preclinical insulinoma imaging (Fig. 2). In vivo PET imaging in nude mice bearing subcutaneous INS-1 xenograft insulinoma tumors demonstrated high binding affinity to GLP-1 and high uptake in insulinomas and pancreas. Tumors on the shoulder indicated by white arrows can be visualized clearly at 1 and 2 h post-injection of ^{18}F-FREM-EM3106B (Fig. 3). The high specific activity

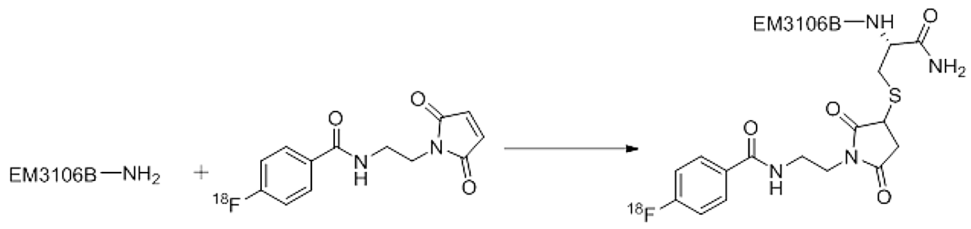

Fig. 2 Scheme of ^{18}F-FBEM-EM3106 radiolabeling (scheme reproduced with permission from Ref. [34])

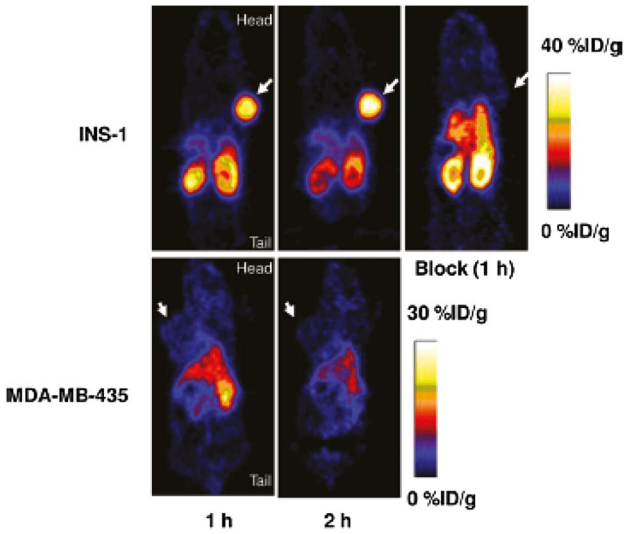

Fig. 3 MicroPET whole body images (coronal plane) of athymic nude mice bearing INS-1 or MDA-MB-435 tumors on the shoulder at 1 and 2 h after tail vein injection of 3.7 MBq of ^{18}F-FBEM-EM3106B. Tumors are indicated by white arrows. The displayed plane was selected to best show the tumor cross-section (figure reproduced with permission from Ref. [34])

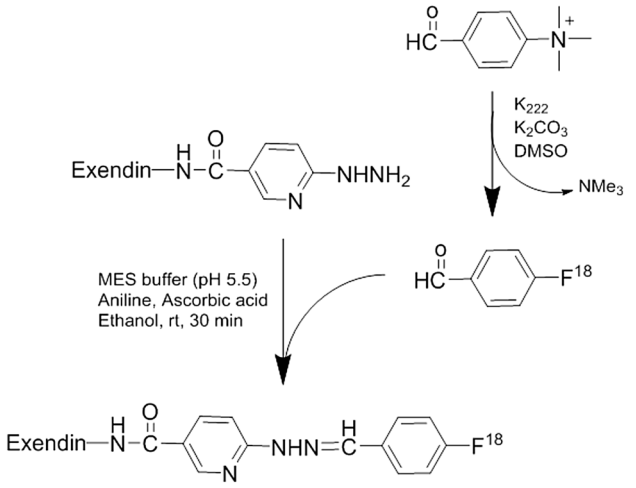

Fig. 4 Scheme of ^{18}F-FBA-exendin(9-39) radiolabelling (scheme reproduced with permission from Ref. [37])

and high tumor uptake of ^{18}F-FREM-EM3106B favour its potential application for clinical insulinoma imaging [34]. ^{18}F-labeled analogues of exendin-4 were developed for PET imaging of GLP-1R in insulinomas [35, 36]. ^{18}F-FBEM-Cys^{40}-exendin-4 was conjugated with cysteine through C-terminal to offer site-specific labeling with ^{18}F-FBEM [35]. The cell uptake and in vivo imaging studies on INS-1 tumor cell and xenograph models showed both high tumor uptake and pancreas uptake, suggested ^{18}F-FBEM-Cys^{40}-exendin-4 could be used as a PET probe for GLP-1-rich tissues. Although both ^{18}F-FREM-EM3106B and ^{18}F-FBEM-Cys^{40}-exendin-4 probes have good tumor uptake, the radiolabelling of these two compounds are time consuming. To improve the radiosynthesis efficiency, a NOTA analogue of exendin-4 with aluminium complexation ^{18}F-AIF-NOTA was developed. Its biological profile was found similar to ^{18}F-FBEM-Cys^{40}-exendin-4 except the much higher kidney uptake [36].

^{18}F-labeled 4-fluorobenzaldehyde, ^{18}F-FBA was conjugated with an exendin(9-39) derivative containing a 6-hydrazinonicotinyl group on the ε-amine of Lys27 through formation of hydrazone to form ^{18}F-FBA-exendin(9-39) as a potential PET probe for pancreatic BCM (Fig. 4) [37]. PET imaging study for pancreatic BCM showed the probe has lack of specific binding to the GLP-1R in pancreas. Derivative of the Lys27 residue might reduce its binding affinity, ^{18}F-labeling on C-terminal of the peptide or other sites rather than Lys27 may improve binding affinity. A new ^{18}F-labeled exendin-4, ^{18}F-TTCO-Cys^{40}-exendin-4 was developed as GLP-1R-targeting probe for imaging transplanted islets [38] (Fig. 5). The tetrazine was conjugated to the exendin-4 through a thiol–maleimide reaction. The resulting tetrazine-Mal-Cys^{40}-exendin-4 reacts with ^{18}F-TCO at 1:1 ratio with a high radiolabelling yield. PET imaging studies on insulinoma INS-1 tumor model showed that ^{18}F-TTCO-Cys^{40}-exendin-4 has a considerable uptake in tumor, and low uptake in kidney (Fig. 6). It also demonstrated that the tracer has a significantly higher uptake into the liver with transplanted human islets in NOD/SCID mice compared to the control mice, indicating high specific binding to GLP-1R.

^{64}Cu-labeling of chelate-conjugated peptides can be used as PET probes for preclinical studies. The positrons derived from ^{64}Cu are low energy which could offer high spatial imaging resolution. Novel ^{64}Cu-labeled exendin-4 probe ^{64}Cu-DO3A-VS-Cys^{40}-exendin-4 for GLP-1R targeting was

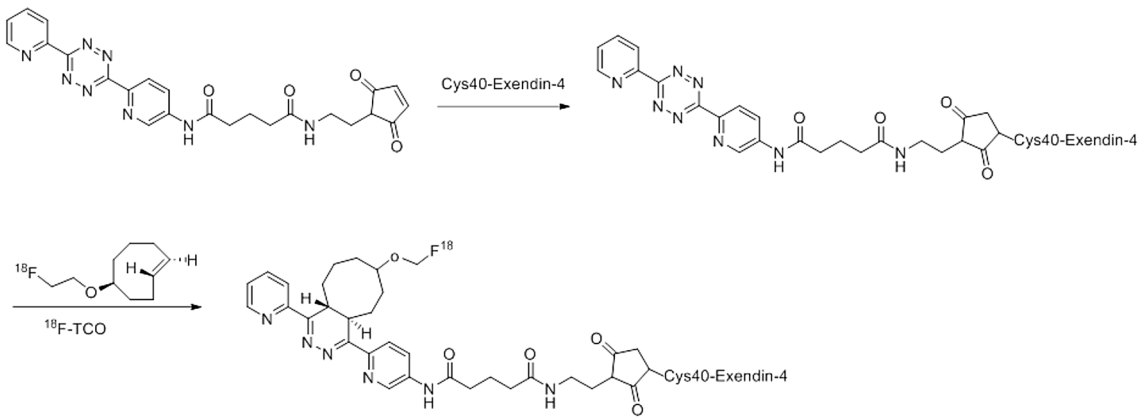

Fig. 5 Scheme of ^{18}F-TTCO-Cys^{40}-exendin-4 radiolabeling (scheme reproduced with permission from Ref. [38])

prepared by conjugation of DO3A-VS (VS = vinylsulfone) with Cys^{40}-exendin-4 [39, 40] (Fig. 7). In vivo imaging on INS-1 tumor model showed high tumor-to-background contrast. The ^{64}Cu-labeling probe also demonstrated specific uptake in the mouse pancreas for intraportal human islet transplantation mouse model, indicating its potential application for in vivo pancreatic islets imaging. Another ^{64}Cu-labeled exendin-4 probe, ^{64}Cu-Lys^{40}-DOTA-NH$_2$-exendin-4 was reported binding specifically to pancreatic islet cells by ex vivo autoradiographic images conducted on rat pancreas sections [41]. Combined with immunohistochemical images, the results suggested it is a potential PET probe for quantitative in vivo measurement of BCM. A new bifunctional chelator NODAGA (NODAGA = 1,4,7-triazacyclononane-1-glutaric acid-4,7-acetic acid) conjugated with exendin-4 was labeled with ^{64}Cu and ^{68}Ga as PET probes for imaging pancreatic islets in rats [42]. ^{64}Cu-labeled NODAGA-exendin-4 has higher GLP-1R specific uptake than its ^{68}Ga-labeled analogue probably because of high specific radioactivity of ^{64}Cu-NODAGA-exendin-4. However, long physical half-life of ^{64}Cu, 12.7 h, leading to substantial residence time of the radionuclide in the kidney cortex and significant radiation burden on the subjects, limits its clinical applications.

^{68}Ga, with a physical half-life of 68 min, is suitable for clinical investigations due to limited radiation burden. Its low cost and easy availability are additional advantages. PET/CT with positron-emitting ^{68}Ga provides potential advantages to SPECT/CT in improved sensitivity, high resolution, fast acquisition time, and accurate quantification.

^{68}Ga-labeled analogues of DO3A-exendin-4 yielded better imaging resolution than imaging with SPECT nuclides such as ^{111}In [43]. ^{68}Ga-DO3A-VS-Cys^{40}-exendin-4 provides simple labeling chemistry and low cost of production. Conjugation of the DO3A chelator does not affect biocompatibility of probe and GLP-1R affinity. ^{68}Ga-DO3A-VS-Cys^{40}-exendin-4 as a PET probe was not only evaluated for imaging of insulinoma tumors [44] and for imaging of GLP-1R in healthy and streptozotocin-induced diabetic pigs [45] but also used to quantify the BCM in the pancreas. The in vivo imaging of GLP-1R with uptake of ^{68}Ga-labeled DO3A-exendin-4 in the pancreas was reported by gradually increasing the dose to quantify the GLP-1R occupancy with a 1-tissue-compartment model in rodents and non-human primates. The uptake of ^{68}Ga-DO3A-VS-Cys^{40}-exendin-4 in the pancreas is liaised with specific receptor binding and decreased by the selective destruction of β-cells.

Receptor-targeting ^{68}Ga-DO3A-VS-Cys^{40}-exendin-4 can be reproducible with high specific radioactivity [44, 45]. Binding studies of ^{68}Ga-DO3A-VS-Cys^{40}-exendin-4 to GLP-1R was evaluated in vitro autoradiography and in vivo. With high affinity to the target, its quantification of GLP-1R is possible. High specific uptake of ^{68}Ga-DO3A-VS-Cys^{40}-exendin-4 was found in GLP-1R-positive tissues such as endocrine INS-1 tumor, pancreas and lung, while low uptake in GLP-1R-negative tissues such as exocrine PANC1 tumor (Fig. 8). The pancreas is difficult to visualize as it is proximal to kidney. In vivo PET/CT imaging demonstrated ^{68}Ga-DO3A-VS-Cys^{40}-exendin-4 has higher tumor-to-background ratio compared with the clinical insulinoma marker [^{11}C]-5-HTP (^{11}C-5-hydroxy-tryptophan) [46]. The serotonin pathway-dependent probe, [^{11}C]-5-HTP uptakes in the β-cell by L-type amino acid transporter converted to serotonin which uptakes in the β-cell by the serotonin transporter or binding to serotonin receptors. But the uptake and metabolism of [^{11}C]-5-HTP in β-cell and exocrine pancreatic cells undergo different pathways [47]. ^{68}Ga-DO3A-VS-Cys^{40}-exendin-4 have also been investigated in streptozotocin-induced diabetic pigs, the results showed that pancreatic uptake of tracer was not reduced by the distinction of β-cells [45]. The first clinical trial using ^{68}Ga-DO3A-VS-Cys^{40}-exendin-4 PET/CT for visualization of GLP-1R in insulinoma and in native pancreas was reported, although the lesions in the histopathological liver could not

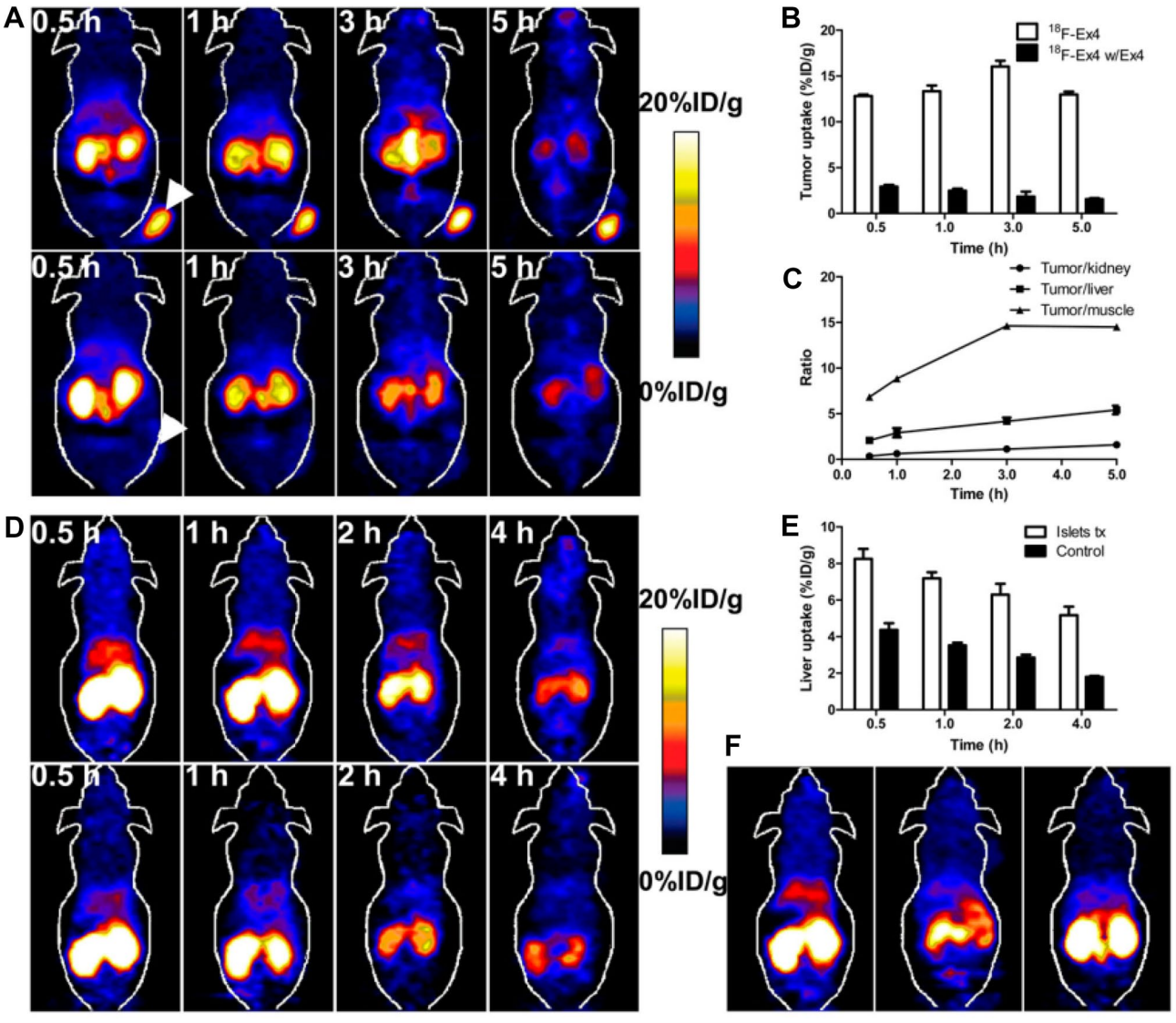

Fig. 6 Representative ^{18}F-TTCO-Cys^{40}-exendin-4 PET images in NOD/SCID mice. **a** Representative microPET images of ^{18}F-TTCO-Cys^{40}-exendin-4 (top) and blocking (bottom) for NOD/SCID mice with INS-1; **b** tumor uptakes between control and blocking groups; **c** tumor to organ ratios of radiotracer at different time points p.i.; **d** representative microPET images of tracer in NOD/SCID mice transplanted with human islets into liver (top) and control mice (bottom) at different time points p.i.; **e** liver uptake between intraportal islet transplantation and sham control groups; **f** microPET images of mice transplanted with human islets (left: control; middle: blocking and sham control mice at 1 h p.i.) (figure reproduced with permission from Ref. [38])

be verified [48]. Recently, PET/CT imaging of the novel chelator NOTA-chelated ^{68}Ga probe, ^{68}Ga-NOTA-exendin-4, correctly detected insulinomas in 42 of 43 patients with high tumor uptake, resulting in sensitivity of 97.7% [49, 50]. The sensitivity is much higher than those of CT, MR and endoscopic ultrasonography. The sensitivities of CT, MR and endoscopic ultrasonography were 74.4, 56.0, and 84.0%, respectively.

Although physical half-life of ^{68}Ga could not lead to long residence time in the kidney cortex, the radiation dose has still been a concern if repeated imaging studies are necessary in humans as low radioactivity associated with the diagnostic examinations could potentially be harmful to healthy tissue after repeated doses. The dosimetry of ^{68}Ga-DO3A-VS-Cys^{40}-exendin-4 was investigated in various subjects based on the biodistribution data in rats, pigs, non-human primates (NHP) and human [51]. The highest accumulation of the tracer is in the kidney, especially in the kidney cortex at all time points for rats, pigs, NHP, and human. The human dosimetry of ^{68}Ga-DO3A-VS-Cys^{40}-exendin-4 has been estimated by extrapolated from the different species. ^{68}Ga-DO3A-VS-Cys^{40}-exendin-4 can be repeatedly administered

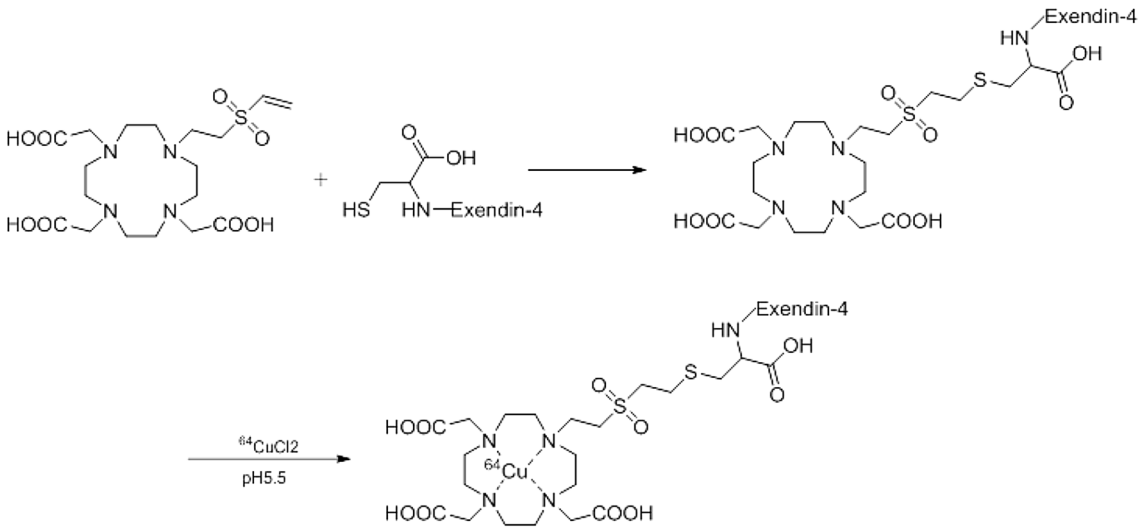

Fig. 7 Synthesis and ^{64}Cu-labeling of ^{64}Cu-DO3A-VS-Cys^{40}-exendin-4 (Ref. [39])

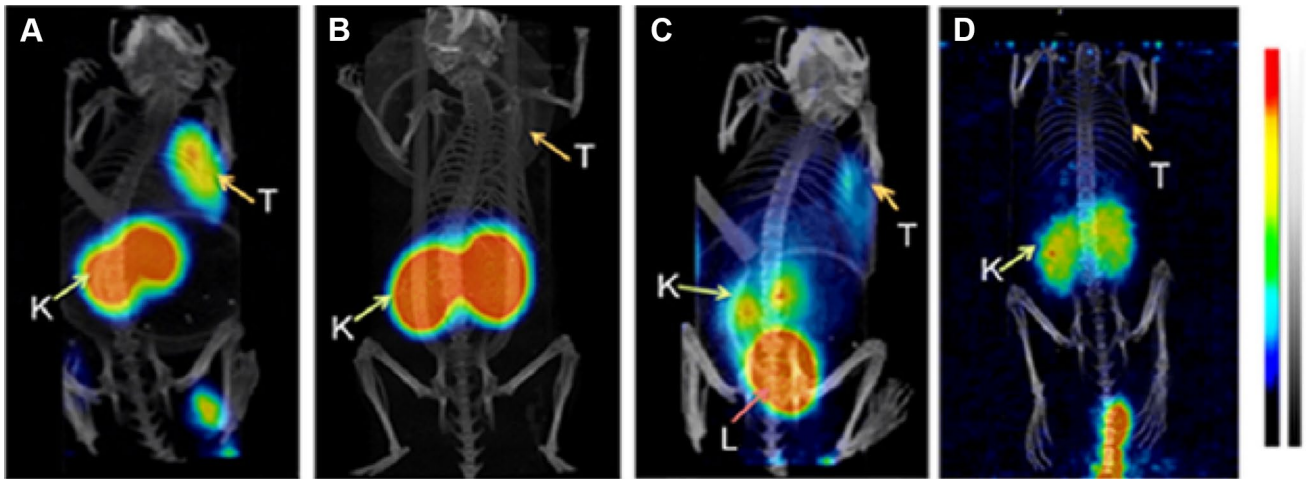

Fig. 8 Representative whole body PET/CT images of INS-1 xenografts, comparing the uptake of ^{68}Ga-DO3A-VS-Cys^{40}-exendin-4 at baseline dose (**a**) and after co-injection of excess precursor peptide (**b**). The animal PET/CT images show that the majority of the ^{68}Ga-DO3A-VS-Cys^{40}-exendin-4 uptake in the tumor was displaceable. Additionally, ^{68}Ga-DO3A-VS-Cys^{40}-exendin-4 has improved tumor to background ratio in a direct within individual comparison with ^{11}C-5-HTP (**c**). PANC1 tumors had significantly low tracer uptake at baseline dose, similar to in the ex vivo organ distribution study (**d**). *T* tumor, *K* kidney and *L* bladder (figure reproduced with permission from Ref. [44])

two to four times per year in human for longitudinal diagnostic studies without exceeding the radiation limits in kidney and other organs.

VMAT2-targeting probes

Type 2 vesicular monoamine transporters (VMAT2) are acidic glycoproteins that translocate monoamines such as dopamine into storage vesicles. VMAT2 are expressed not only in the monoaminergic neurons which are in charge of the uptake of cytosolic monoamines into synaptic vesicles but also in β-cells of the pancreas [52–54]. VMAT2 in β-cells is capable of controlling vesicular monoamine content. The VMAT2 imaging can be used for investigating the relationship between loss of β-cells in association with insulin and initiation of diabetes mellitus [55, 56].

Tetrabenazine is a relatively specific inhibit of VMAT2. Dihydrotetrabenazine (DTBZ) and other small molecules which are highly selective for VMAT2 have been developed as PET probes for VMAT2 [57]. DTBZ and its analogue PET probes demonstrated much higher affinity to VMAT2

than to VMAT1 [58]. ^{11}C-DTBZ was first synthesized in 1993 [59]. Various labeling methods of ^{11}C-tetrabenazine and its methoxy derivatives were used for imaging VMAT2 in dopaminergic neurons within mouse brain [60–63]. Binding of α-DTBZ to the vesicular monoamine transporter is stereospecific [64]. There are two enantiomers of α-DTBZ, and only (+)-α-DTBZ showed selective and high affinity for the vesicular monoamine transporter.

^{11}C-DTBZ has been used for visualizing BCM of endocrine pancreas to discriminate differences in probe uptake among streptozotocin-induced diabetic rats and those with chemically induced diabetes. Decreased probe uptake within the pancreas of rodents with streptozotocin-induced diabetes is related to their euglycemic historical controls [65]. (+)-α-DTBZ has been applied for imaging VMAT2 in the pancreas of various species [66, 67]. ^{11}C-DTBZ PET of pancreas was performed clinically in long-standing T1D and healthy subjects. Time-activity curves in the pancreas and left renal cortex demonstrated excellent tracer uptake in the pancreas for both patients and healthy subjects with peaking at around 10 min and a relatively quick washout for both groups [66] (Fig. 9). There is no difference between imaging of normal and patients with long-standing T1D because of the presence of VMAT2 binding signal in TID pancreas. When renal cortex was employed as a reference to evaluate ^{11}C-DTBZ nonspecific binding in pancreas, the nonspecific ^{11}C-DTBZ binding could be higher in human pancreas than in the renal cortex as VMAT2 expression is undetectable in the renal cortex, thus the nonspecific binding in the pancreas would be underestimated. The probe uptake in the renal cortex is considerable with a quick washout, while uptake in the liver slowly increases throughout the experiment. The overall time course of ^{11}C-DTBZ uptake in pancreas and renal cortex showed tracer uptake in these two organs is reversible. ^{11}C-DTBZ is catabolized by glucuronidation in the liver and excreted from bile and urine. VMAT binding potential and functional binding capacity seems to overestimate BCM in long-standing T1D possibly because of higher nonspecific binding in the pancreas than in renal cortex. Nonspecific binding of ^{11}C-(+)-DTBZ in human pancreas would hinder its clinical applications. It implicated the regulation of VMAT2 gene expression, the mechanisms of its function in β-cell need to be explored before using VMAT2 measurements as a diagnostic tool [67].

To improve its application in BCM, ^{18}F-labeled DTBZ was developed since ^{18}F radioisotope has longer half-life

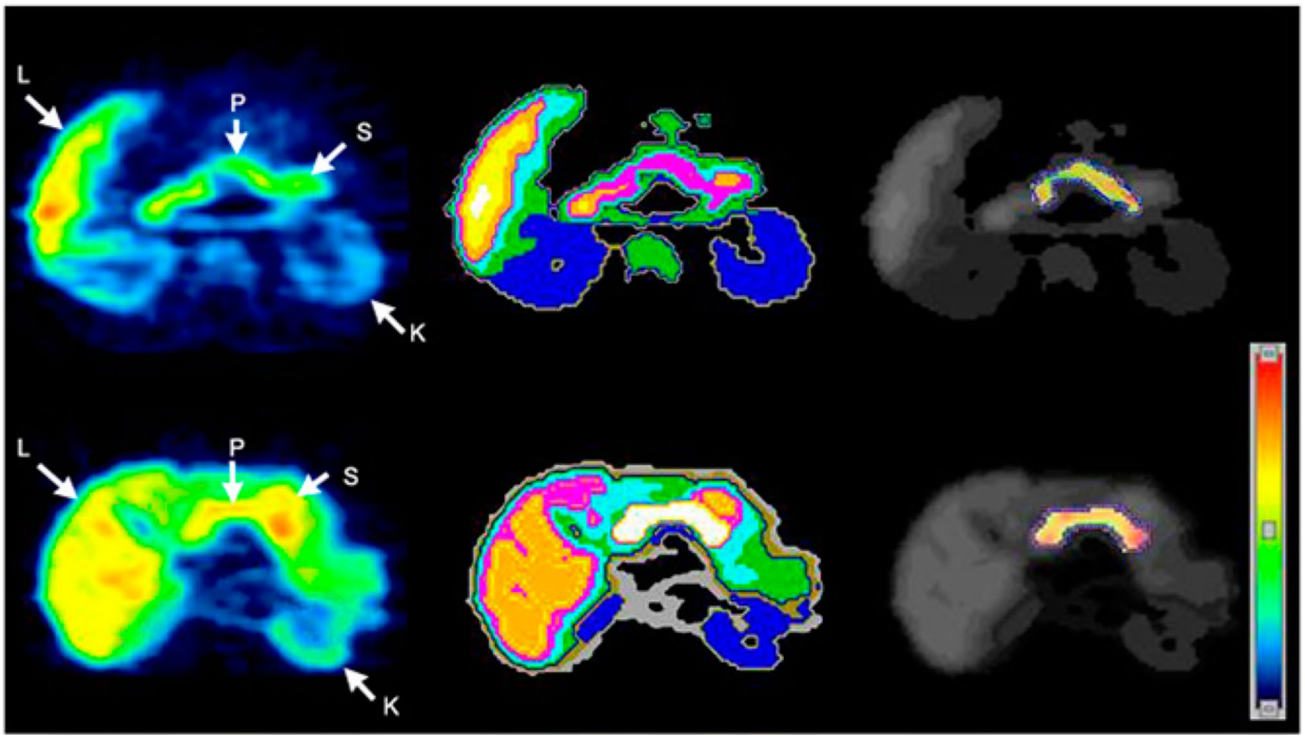

Fig. 9 Transverse ^{11}C-dihydrotetrabenazine PET images of patients (top row) and controls (bottom row). Summed dynamic PET images were obtained 0-90 min after injection of approximately 481–555 MBq of ^{11}C-dihydrotetrabenazine (left). Corresponding tissue segmentation images are also shown (middle), with different colours being used to represent different organs. Voxelwise parametric images of VMAT2-binding potential (BP_{ND}) are shown (right) using another color scale (right bottom). These BP_{ND} images are fused onto segmentation image using grayscale, with pancreatic ROI boundary shown using dotted blue outlines (right). L 5 liver; K 5 kidney; S 5 stomach; P 5 pancreas (figure reproduced with permission from Ref. [66])

and higher electronegativity than those of ^{11}C. There are two types of derivatives, ^{18}F epoxide derivative of DTBZ ^{18}F-fluoroepoxide-DTBZ [68] and ^{18}F alkyl derivative of ^{18}F-fluoroalkyl-DTBZ [69–73] (Fig. 10). The ^{18}F-fluoroepoxide-DTBZ is highly selective binding to VMAT2, the in vivo biodistribution of ^{18}F-fluoroepoxide-DTBZ of rats demonstrated significant uptake in pancreas (5% ID/g at 30 min p.i; 2.68%ID/g at 60 min p.i.) and low uptake in the livers, a higher pancreas-to-liver ratio compared to its alkyl derivatives. The new extraction pattern is likely because of hydrolysable epoxide group [68]. ^{18}F-fluoroepoxide-DTBZ has high pancreatic uptake in healthy rats.

A novel ^{18}F-fluoropropyl derivative ^{18}F-FP-(+)-DTBZ was developed to evaluate VMAT2 pancreatic binding by PET [69]. The obtained preliminary data with ^{18}F-FP-(+)-DTBZ showed good pancreas specificity and potential for quantitative measurement of VMAT2 binding sites. Pancreatic uptake of ^{18}F-FP-(+)-DTBZ in T1D patients was substantially lower than that of control subjects, Considerably less ^{18}F-FP-(+)-DTBZ binding density in T1D subjects was found than in healthy controls [70]. Compared with its ^{11}C-labeled derivative, ^{18}F-FP-(+)-DTBZ significantly improved dynamic range of pancreatic binding parameters correlating with β-cell function. The functional loss of β-cell density in T1D patients was thus distinguishable. Although specific high-affinity binding of these VMAT2 targeted radioligand to VMAT2 in β-cell is confirmed, there are substantial specific and nonspecific bindings which could limit the BCM quantification [71]. Background binding characteristics of ^{18}F-FP-(+)-DTBZ in rat pancreas demonstrated there is nonspecific binding to sigma receptors present in both endocrine and exocrine cells of pancreas. It could lead to a significant background noise for quantitating BCM [72]. ^{18}F-FP-DTBZ showed considerably specific VMAT2 binding in both the pancreas and striatum in baboons was reported [73]. The non-displaceable VMAT2 binding of (+) and (−) enantiomers of ^{18}F-FP-DTBZ within the baboon pancreas was also investigated. The overestimation of BCM with ^{18}F-FP-(+)-DTBZ PET imaging could be contributed by two factors: small percentages of VMAT-positive pancreatic polypeptide-producing cells and a weak affinity for sigma receptor of ^{18}F-FP-(+)-DTBZ. Directly, measurement of non-displaceable binding in the healthy human and T1D patient pancreas by (*R*) and (*S*) enantiomers could explain the overestimation of BCM in T1D.

The 9-^{18}F-fluoroethyl-(+)-dihydrotetrabenazine (^{18}F-FE-(+)-DTBZ) was found to be high specific binding to VMAT2. But there is high non-displaceable binding to exocrine tissue. The probe metabolized extensively by in vivo defluorination in a large piglet model [74]. Deuterated analogue of ^{18}F-FE-(+)-DTBZ was designed to improve the in vivo stability which could improve the VMAT2 uptake in BCM [75]. ^{18}F-FE-DTBZ-d4 was synthesized in two steps following the indirect fluorination method with slight modifications [76]. The in vitro and in vivo results of deuterated FE-DTBZ-d4 were compared retrospectively to that of the non-deuterated FE-DTBZ probe. The in vivo PET/CT piglet studies showed homogeneous uptake of the

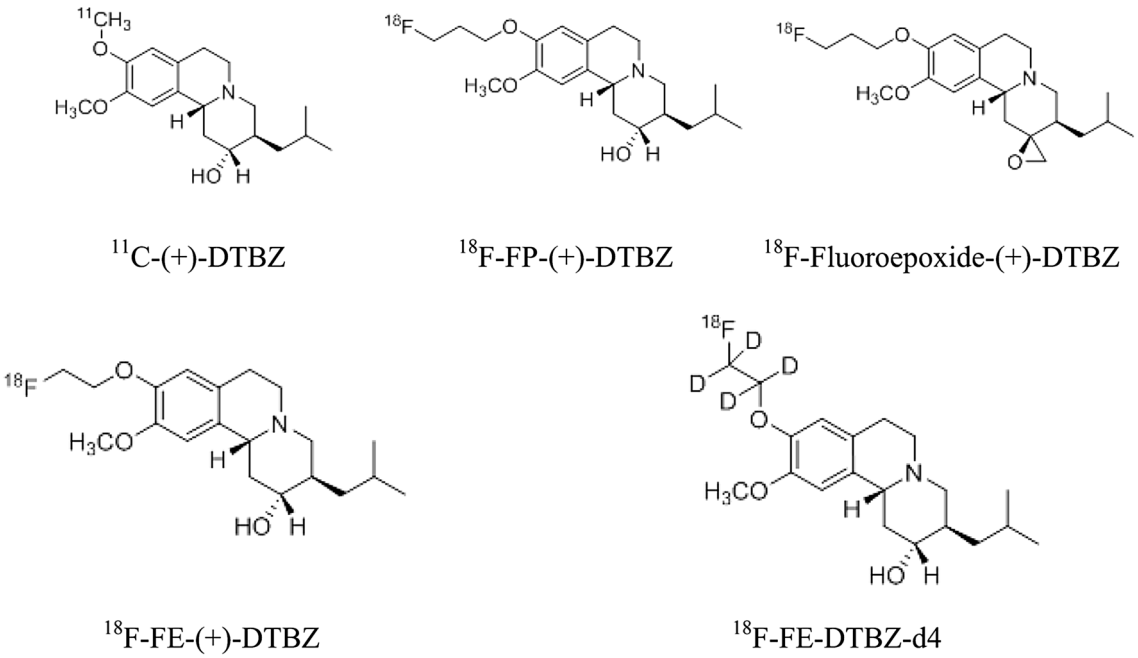

Fig. 10 Schematic structures of ^{11}C- and ^{18}F-labeled DTBZ probes

^{18}F-FE-DTBZ-d4 in the pancreas. The average uptake of ^{18}F-FE-DTBZ-d4, expressed in SUV, reached 2.64 shortly after the I.V. administration with a SUV of 1.8 after 90 min, which was comparable to that of the non-deuterated version. Notable accumulation was observed in the liver and spleen with faster washout kinetics than the pancreas. Apart from the excretion via the bile system, excretion via the kidney, bladder and urethra was also observed (Fig. 11(I)). The main goal of the study was achieved by observing reduced bone uptake of the deuterated tracer ^{18}F-FE-DTBZ-d4 in vivo, where it showed moderate uptake (SUV 1.4) of radioactivity with no further accumulation (Fig. 11(II)), whereas the bone uptake increased linearly with time for the non-deuterated analogue (SUV of 3.1 at 90 min). However, there was no significant difference observed in specific VMAT2 binding uptake in the pancreas in in vivo PET/CT studies, even though more native ^{18}F-FE-DTBZ-d4 was present in blood plasma.

Other than ^{11}C and ^{18}F PET nuclides, currently there is only one report using ^{64}Cu-specific bifunctional chelator CB-TE2A for the probe development of DTBZ targeting imaging. ^{64}Cu-labeled CB-TE2A conjugation with (±)-DTBZ, ^{64}Cu-CB-TE2A-(+)-DTBZ and ^{64}Cu-CB-TE2A-(−)-DTBZ were synthesized [77]. Ex vivo binding assay of ^{64}Cu-CB-TE2A-(+)-DTBZ exhibited the desired preferential accumulation in freshly isolated porcine islets, while the VMAT2-specific binding of ^{64}Cu-CB-TE2A-(−)-DTBZ is low, similar to ^{11}C- or ^{18}F-labeled (±) DTBZ. The conjugation of (+)-DTBZ to CB-TE2A moiety did not compromise the VMAT2-specific binding affinity.

GPR44-targeting probes

G-protein-coupled receptor 44 (GPR44) known as prostaglandin D2 receptor 2, has been characterized as a highly β-cell-specific surface marker [78]. The expression and density of GPR44 protein in endocrine isolated from human islets and exocrine tissues were recently assessed by a ^{3}H-labeled GPR44 probe ^{3}H-AZD3825 [79]. The possibility of GPR44 to be used as a surrogate biomarker was also evaluated by comparing directly with a ^{3}H-labeled ^{3}H-DTBZ which has a high affinity for VMAT2. The specific binding of ^{3}H-DTBZ was much higher than that of ^{3}H-AZD3825 in both endocrine and exocrine tissues. ^{3}H-AZD3825 and ^{3}H-DTBZ showed similar specificity for endocrine tissue (56 ± 3 and 49 ± 5%, respectively), but specific binding of ^{3}H-DTBZ (22 ± 2%) to exocrine tissue was almost 3 times

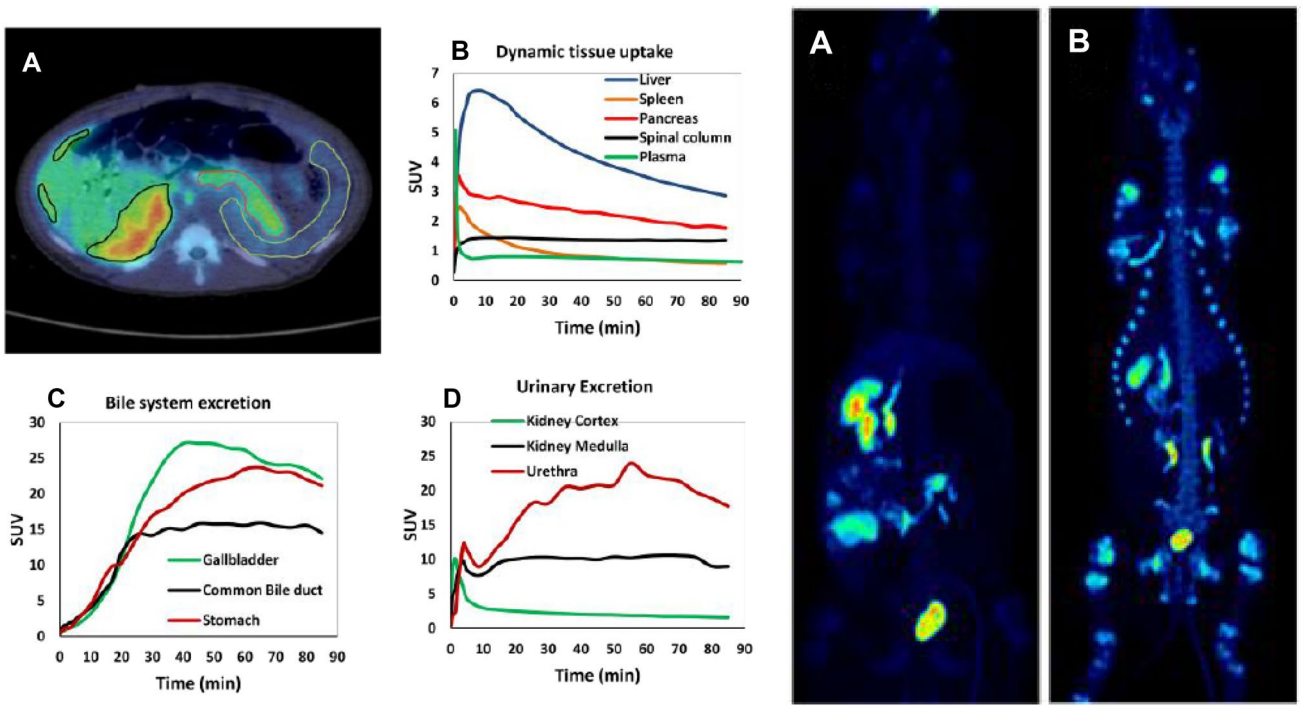

Fig. 11 I Delineation of pancreas (red), spleen (green) and parts of the anterior and posterior hepatic segments (black) exemplified on a transaxial PET/CT fusion image (**a**). The average dynamic uptake of ^{18}F-FE-DTBZ-d4 in pancreas and other abdominal tissues from four different piglets (**b**). Excretion through the biliary system is the fate of a majority of the tracer and its metabolites (**c**), but there is also elimination of tracer by urine (**d**). II 3D maximum intensity projection (MIP) 90 min after administration of a ^{18}F-FE-DTBZ-d4, low accumulation in bone structures indicates low levels of free ^{18}F^{-}. b Non-deuterated ^{18}F-FE-DTBZ, high accumulation in bone structures due to higher levels of free ^{18}F^{-}. Colours indicate SUV 0 (black) to SUV 30 (white) (figure reproduced with permission from Ref. [76])

higher than that of ^{3}H-AZD3825 (6.3 ± 2%). The specific binding of ^{3}H-DTBZ was approximately 2.2 times higher in endocrine tissue than in exocrine tissue, while it was almost 20 times higher for ^{3}H-AZD3825. However, the specific binding of ^{3}H-AZD3825 was significantly higher for EndoC-bH1 cells compared to endocrine tissue, while the specific binding of ^{3}H-DTBZ was almost same in endocrine tissue and in EndoC-bH1 cells. In addition, the uptake ratio between β-cells and the exocrine tissue was almost 90 times for ^{3}H-AZD3825. Both ^{3}H-AZD3825 and ^{3}H-DTBZ showed negligible specificity towards the homogenates of INS-1 insulinoma xenografts. The saturation binding experiment displayed the affinity of ^{3}H-DTBZ in endocrine and exocrine tissues were almost 6 and 9 times lower compared to that of ^{3}H-AZD3825. RNA analysis found transcript levels of GPR44 in islets were much higher than in exocrine tissue. The consistency of GPR44 expression in both endocrine and exocrine pancreatic tissues among individuals suggested it could be potentially used as a dependable and precise biomarker for BCM imaging.

^{11}C- and ^{3}H-labeled novel probes ^{11}C-AZ Compound X and ^{3}H-AZ Compound X were synthesized and evaluated as probes for in vitro binding properties against human and rat pancreatic tissue slices and tissue homogenates [80]. β-particles (electrons) emitting ^{3}H isotope is not useful for non-invasive imaging of living subjects as electrons do not travel significant distances, it is suitable for autoradiography. The autoradiography images using ^{11}C-AZ Compound X in human pancreatic slices showed heterogeneous hotspots corresponding to islets of Langerhans in both healthy and T2DM subjects. The selective affinity of ^{11}C-AZ Compound X towards GPR44 was further confirmed with rat pancreatic slice which lacks GPR44 expression as negative control. The autoradiography images of rat pancreatic slice do not show any heterogeneous hotspots in contrast to human pancreatic slices. The specific affinity of probe was also confirmed by co-incubation with 20 μM GPR44 antagonist. The results showed that the GPR44 antagonist could able to completely block the binding of probe to human pancreatic tissue in contrast with rat pancreatic tissue. The islet hotspots showed more than seven times higher binding toward ^{11}C-AZ Compound X compared to the exocrine tissues for both healthy and T2DM subjects (Fig. 12). ^{3}H-AZ Compound X also provides similar in vitro autoradiography. In vitro binding of ^{11}C-AZ Compound X to pancreatic tissue homogenates showed the specific binding was 8–20 times higher in pancreatic islets than in exocrine tissue. The in vitro binding properties of GPR44 probe, ^{11}C/^{3}H-AZ Compound X, in human pancreas and rat pancreas showed very promising results. These results motivated further evaluation as PET probes for preclinical application. The specific binding of ^{11}C-AZ Compound X against the β-cells in pancreatic islet was established by insulin antibody staining. Most of the hotspots showed significant co-localisation with antibody signal. The in vitro results are quite promising for both ^{3}H/^{11}C-AZ Compound X in both human and rat pancreatic tissues. However, it required systematic preclinical studies to assure they could be used as probes for quantifying BCM in vivo.

Antigen-targeting probes

Antigen expressed in β-cells to a certain degree. Autoantigenic target is potential target of the immune system, with downstream implications for the etiology of T1D [81]. A ^{111}In-labeled β-cell-specific monoclonal antibody IC2, ^{111}In-DTPA-IC2 was synthesized to investigate its potential antigen probe for BCM in normal and diabetic states [82]. IC2 is well known to bind specifically to the cell membrane of β-cells. The probe showed specific binding to β-cells with a negligible binding to exocrine pancreas. SPECT imaging exhibited significant difference in signal intensity between normal and diabetic pancreases. A direct correlation between accumulation of the probe with BCM in normal and diabetic animals was also found. Successful preclinical studies contribute to further development of the probe for quantifying BCM in diabetic diagnosis clinically.

A ^{125}I-labelled monoclonal antibody ^{125}I-γ-G was used as a potential SPECT imaging probe for pancreatic β-cells [83]. ^{125}I-γ-G displayed almost one-fold higher binding in isolated pancreatic islets than in acinar tissue. However, no significant difference between the tissues from control and streptozotocin diabetic rats was identified. The result suggested the uptake of this probe was not able to reflect a reduction in the number of β-cell in the diabetic pancreas. These findings indicated that ^{125}I-γ-G might not be a promising probe for selective SPECT imaging of the endocrine pancreas.

Glucokinase targeting probes

Glucokinase, an enzyme mostly expressed in β-cells of pancreatic islets of Langerhans and hepatocytes in the liver, is one of the potential targets for in vivo imaging of BCM. Recently ^{11}C-labeled ^{11}C-AZ12504948, a glucokinase activator was evaluated for preclinical PET imaging of glucokinase [84]. From both the autoradiography of human tissues and PET/CT images of pig and cynomolgus monkey, the probe identified certain specificity for glucokinase in liver, but not in pancreas because of low specific uptake in pancreas. The probe required further structural modifications to improve its target specificity so that it could be used as an in vivo PET imaging probe for glucokinase.

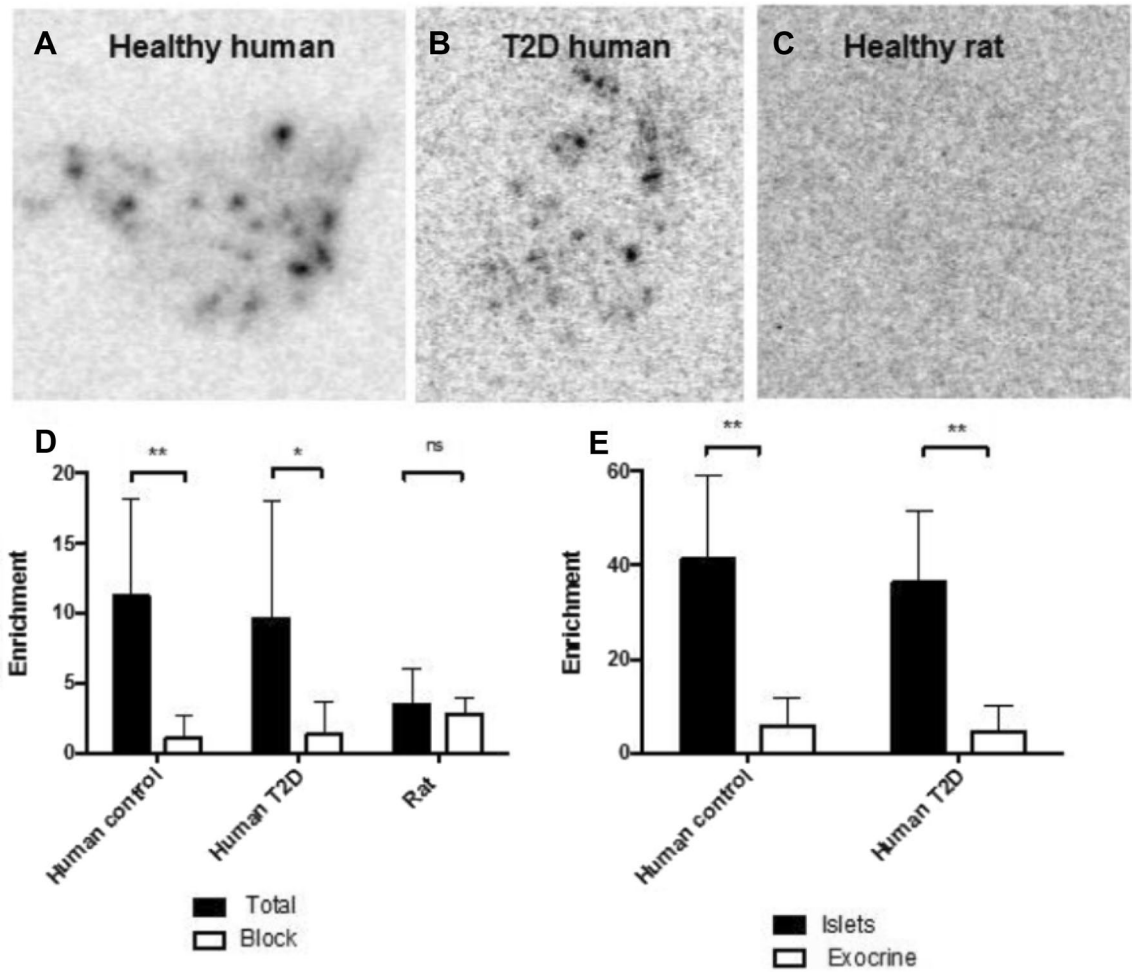

Fig. 12 In vitro autoradiography of ^{11}C-AZ Compound X, Specific binding in pancreas from healthy human subjects (**a**), subjects with T2D (**b**) and healthy rat (**c**). The pancreatic binding of tracer is displaceable in human but not in rat (**d**), and the human pancreatic binding is concentrated to the islet of Langerhans (**e**) (figure reproduced with permission from Ref. [80])

Reporter gene-targeting probes

The approach of PET imaging through the cell engineering with reporter genes that retain the PET probe in the cell has commonly been used to track the function and location of transplanted cells in various disease models. The most widely used reporter genes for PET imaging are HSV1-TK and its derivative HSV1-sr39tk [85]. FHBG is a known nucleoside derivative which is metabolized by HSV1-TK and sr39tk [86–88]. After the injection, the ^{18}F-labeled FHBG, the probes are transported to the cells where it gets phosphorylated, and metabolically trapped in cells expressing the reporter gene. The accumulated metabolites of ^{18}F-labeled probe could be detected by PET.

The generation and characterization of the MIP-sr39tk mouse to image of endogenous pancreatic islets using PET were investigated. The ex vivo studies revealed that there is a 4.5-fold higher uptake of ^{18}F-FHBG in the pancreas of the transgenic mice compared with the non-transgenic one [89]. The results suggested that higher retention of the ^{18}F-FHBG occurred because of expression of sr39TK in transgenic mouse. The significant correlation between islet number and ^{18}F-FHBG uptake was observed. It also indicated that MIP-sr39tk mouse model could be used for in vivo imaging of BCM.

Discussion

With PET imaging alone, there is limited anatomical reference frame, difficult to outline the anatomic structure of pancreas which situate next to abdominal region. The limitation could overcome by combining PET with CT. PET/CT is high sensitive imaging methodology, with a target-specific tracer, can serve as a non-invasive tool to monitor the decline in the viable number of β-cell and the fate of transplanted cells, to

detect the post-transplantation islet loss. It is an advantage to the indirect method to measure patient's exogenous insulin as the insulin secretory capacity of beta cells is not always consistent under various physiologic conditions [90, 91].

Although it has been shown that SPECT/CT is a very sensitive, non-invasive imaging technique to localized insulinomas using GLP-1R targeting such as [Lys^{40}(Ahx-HYNIC-^{99m}Tc/EDDA)NH$_2$]exendin-4, and radiochemistry with technetium is advanced, cheap and readily available, but the significantly lower tumor and organ uptakes lead to the significantly less efficient internalization. PET/CT has a higher spatial resolution and sensitivity when compared with SPECT/CT [92]. PET/CT quantifies the tracer uptake more accurately [93]. The other example is ^{68}Ga-DOTA-exendin-4 PET/CT correctly identified the insulinoma in 4 of 4 patients, whereas ^{111}In-DOTA-exendin-4 SPECT/CT correctly identified the insulinoma in only 2 of 4 patients [33].

β-Cells are low, only 1–2% in abundance, and are dispersed throughout the pancreas. BCM PET has a potential limitation due to its limited spatial resolution. For GLP-1R study, considerably overlap between groups of normal healthy subjects and subjects with T1D was noticed [94]. The estimation of serotonergic biosynthesis by DOPA decarboxylase in pancreas by PET allows discriminating non-diabetic subjects from subjects with T1D without significant overlap. However, the serotonergic biosynthesis pathway is not specific to the β-cells and it is present in all pancreatic endocrine [47].

For ^{11}C-DTBZ PET study, patients with long-standing T1D are expected to have almost total loss of β-cells, however, it was observed that ^{11}C-DTBZ-binding potential only decreases around 15% of the value in control subjects [66]. The calculated functional binding capacity BP_{ND} seems to overrate the BCM due to high nonspecific binding in the pancreas. This residual signal in T1D pancreas may possibly generate from the VMAT2 expressed within the pancreas but not associated with the BCM (e.g., neuronal cells or immature b-cells). In addition, it was reported that almost one in two pancreatic polypeptide cells are VMAT2 positive. In general, VMAT2 has a close relationship with BCM but its expression is not completely restricted to β-cells because small percentages of polypeptide cells, as well as the innervation, are VMAT2 positive [55, 95, 96]. Non-VMAT2 binding of ^{11}C-DTBZ to exocrine pancreas exceeds VMAT2 binding to β-cells was reported [97]. In vitro autoradiography of human pancreas also suggested that a large portion of DTBZ binding mostly represents the nonspecific binding. The specific binding of the tracer to the islet did not satisfactorily surpass the nonspecific binding in the exocrine pancreatic tissue which restricts its use to quantify BCM in vivo [74]. The expression of GPR44 receptor is highly specific for β-cells rather than exocrine and other endocrine cells, it has relatively low densities compared to VMAT2 in the endocrine pancreas. Hence, it is difficult to get a strong enough signal for in vivo quantification of BCM [98].

The PET tracer uptakes are different among the species because of different kinetics and washout. The magnitude of PET signal in human T1D patient pancreas is not the same as the one in diabetic pancreas of rodent models. The affinity for BCM, pathophysiology, therapeutic interventions need to be further studied to explain these differences. Proposing the probe with high target affinity and low nonspecific binding would be the future direction.

Conclusion

The goal of PET probe development for imaging pancreatic islet cells is to develop radioligands which have the following characteristics: high specific target binding with low nonspecific binding in surrounding tissue, optimal biodistribution and pharmacokinetic profile with nontoxic to islet. The demand for new PET probes for imaging pancreatic islet cells especially β-cell in preclinical and clinical investigations is expected to increase to achieve this goal. This review provides comprehensive overview of noteworthy probes which are proteins targeting including GLP-1, VMAT2, GPR44, antigen, glucokinase and reporter genes in the beta cell. New potential candidates including tritium-3, carbon-11, fluorine-18-, gallium-68-, copper-64- and indium-11- (for SPECT)-labeled radioligands have been evaluated in rodents, pigs, non-human primates and humans. In the meantime, the various issues of targeting probes have been addressed. The ideal PET probes for accurate and non-invasive imaging for pancreatic islet cells need to be developed. The PET/MR bimodality imaging approach could be the way for the future studies for imaging pancreatic islet cells especially β-cell. The review could offer some future research directions for this emerging field to those who expertise in medicinal chemistry and radiochemistry, spectroscopy, biology, radiology and biomedical imaging engineering.

Acknowledgements Authors acknowledge the support from Lee Kong Chian School of Medicine, Nanyang Technological University (NTU) Start-Up Grant, Singapore and NTU Austrian Institute of Technology and Medical University of Vienna internal Grant (NAM/15005), Singapore.

Author contributions CTY: Literature search and review, manuscript writing. KKG: Literature search and review, manuscript writing. PP: Content planning and editing. OL: Content planning and editing. JL: Content planning and editing. CH: Content planning and editing. BG: Content planning and editing.

Compliance with ethical standards

Conflict of interest CTY declares that he has no conflict of interest. KKG declares that he has no conflict of interest. PP declares that he has no conflict of interest. OL declares that he has no conflict of interest. JL declares that he has no conflict of interest. CH declares that he has no conflict of interest. BG declares that he has no conflict of interest.

Ethical approval This article does not contain any studies with human participants or animal performed by any of the authors.

References

1. Pisania A, Weir GC, O'Neil JJ, Omer A, Tchipashvili V, Lei J, Colton CK, Bonner-Weir S (2010) Quantitative analysis of cell composition and purity of human pancreatic islet preparations. Lab Invest 90(11):1661–1675. doi:10.1038/labinvest.2010.124
2. Brissova M, Fowler MJ, Nicholson WE, Chu A, Hirshberg B, Harlan DM, Powers AC (2005) Assessment of human pancreatic islet architecture and composition by laser scanning confocal microscopy. J Histochem Cytochem 53(9):1087–1097. doi:10.1369/jhc.5C6684.2005
3. Bosco D, Armanet M, Morel P, Niclauss N, Sgroi A, Muller YD, Giovannoni L, Parnaud G, Berney T (2010) Unique arrangement of alpha- and beta-cells in human islets of Langerhans. Diabetes 59(5):1202–1210. doi:10.2337/db09-1177
4. Rahier J, Guiot Y, Goebbels RM, Sempoux C, Henquin JC (2008) Pancreatic beta-cell mass in European subjects with type 2 diabetes. Diabetes Obes Metab 10(Suppl 4):32–42. doi:10.1111/j.1463-1326.2008.00969.x
5. Scully T (2012) Demography: to the limit. Nature 492(7427):S2–S3. doi:10.1038/492S2a
6. Gepts W (1965) Pathologic anatomy of the pancreas in juvenile diabetes mellitus. Diabetes 14(10):619–633. doi:10.2337/diab.14.10.619
7. Butler AE, Janson J, Soeller WC, Butler PC (2003) Increased β-cell apoptosis prevents adaptive increase in β -cell mass in mouse model of type 2 diabetes: evidence for role of islet amyloid formation rather than direct action of amyloid. Diabetes 52(9):2304–2314. doi:10.2337/diabetes.52.9.2304
8. Melendez-Ramirez LY, Richards RJ, Cefalu WT (2010) Complications of type 1 diabetes. Endocrinol Metab Clin North Am 39(3):625–640. doi:10.1016/j.ecl.2010.05.009
9. Matveyenko AV, Butler PC (2008) Relationship between beta-cell mass and diabetes onset. Diabetes Obes Metab 10 (Suppl. 4):23-31. doi:10.1111/j.1463-1326.2008.00939.x
10. Krogvold L, Edwin B, Buanes T, Frisk G, Skog O, Anagandula M, Korsgren O, Undlien D, Eike MC, Richardson SJ, Leete P, Morgan NG, Oikarinen S, Oikarinen M, Laiho JE, Hyoty H, Ludvigsson J, Hanssen KF, Dahl-Jorgensen K (2015) Detection of a low-grade enteroviral infection in the islets of langerhans of living patients newly diagnosed with type 1 diabetes. Diabetes 64(5):1682–1687. doi:10.2337/db14-1370
11. Berney T, Toso C (2006) Monitoring of the islet graft. Diabetes Metab 32(5 Pt 2):503–512. doi:10.1016/S1262-3636(06)72803-8
12. Leoni L, Roman BB (2010) MR imaging of pancreatic islets: tracking isolation, transplantation and function. Curr Pharm Des 16(14):1582–1594. doi:10.2174/138161210791164171
13. Medarova Z, Moore A (2009) MRI as a tool to monitor islet transplantation. Nat Rev Endocrinol 5(8):444–452. doi:10.1038/nrendo.2009.130
14. Medarova Z, Moore A (2009) MRI in diabetes: first results. Am J Roentgen 193(2):295–303. doi:10.2214/AJR.08.2156
15. Virostko J, Radhika A, Poffenberger G, Chen Z, Brissova M, Gilchrist J, Coleman B, Gannon M, Jansen ED, Powers AC (2010) Bioluminescence imaging in mouse models quantifies beta cell mass in the pancreas and after islet transplantation. Mol Imaging Biol 12(1):42–53. doi:10.1007/s11307-009-0240-1
16. Roth DJ, Jansen ED, Powers AC, Wang TG (2006) A novel method of monitoring response to islet transplantation: bioluminescent imaging of an NF-kB transgenic mouse model. Transplantation 81(8):1185–1190. doi:10.1097/01.tp.0000203808.84963.13
17. Halldin C, Gulyas B, Farde L (2001) PET studies with carbon-11 radioligands in neuropsychopharmacological drug development. Curr Pharm Des 7(18):1907–1929. doi:10.2174/1381612013396871
18. Di Gialleonardo V, de Vries EF, Di Girolamo M, Quintero AM, Dierckx RA, Signore A (2012) Imaging of beta-cell mass and insulitis in insulin-dependent (Type 1) diabetes mellitus. Endocr Rev 33(6):892–919. doi:10.1210/er.2011-1041
19. Sweet IR, Cook DL, Lernmark A, Greenbaum CJ, Krohn KA (2004) Non-invasive imaging of beta cell mass: a quantitative analysis. Diabetes Technol Ther 6(5):652–659. doi:10.1089/dia.2004.6.652
20. Blomberg BA, Codreanu I, Cheng G, Werner TJ, Alavi A (2013) Beta-cell imaging: call for evidence-based and scientific approach. Mol Imaging Biol 15(2):123–130. doi:10.1007/s11307-013-0620-4
21. Laurent D, Vinet L, Lamprianou S, Daval M, Filhoulaud G, Ktorza A, Wang H, Sewing S, Juretschke HP, Glombik H, Meda P, Boisgard R, Nguyen DL, Stasiuk GJ, Long NJ, Montet X, Hecht P, Kramer W, Rutter GA, Hecksher-Sorensen J (2016) Pancreatic beta-cell imaging in humans: fiction or option? Diabetes Obes Metab 18(1):6–15. doi:10.1111/dom.12544
22. Karlsson F, Antonodimitrakis PC, Eriksson O (2015) Systematic screening of imaging biomarkers for the Islets of Langerhans, among clinically available positron emission tomography tracers. Nucl Med Biol 42(10):762–769. doi:10.1016/j.nucmedbio.2015.06.004
23. Wu Z, Kandeel F (2010) Radionuclide probes for molecular imaging of pancreatic beta-cells. Adv Drug Deliv Rev 62(11):1125–1138. doi:10.1016/j.addr.2010.09.006
24. Li J, Karunananthan J, Pelham B, Kandeel F (2016) Imaging pancreatic islet cells by positron emission tomography. World J Radiol 8(9):764–774. doi:10.4329/wjr.v8.i9.764
25. Manandhar B, Ahn JM (2015) Glucagon-like peptide-1 (GLP-1) analogs: recent advances, new possibilities, and therapeutic implications. J Med Chem 58(3):1020–1037. doi:10.1021/jm500810s
26. Tornehave D, Kristensen P, Romer J, Knudsen LB, Heller RS (2008) Expression of the GLP-1 receptor in mouse, rat, and human pancreas. J Histochem Cytochem 56(9):841–851. doi:10.1369/jhc.2008.951319
27. Reubi JC, Waser B (2003) Concomitant expression of several peptide receptors in neuroendocrine tumours: molecular basis for in vivo multireceptor tumour targeting. Eur J Nucl Med Mol Imaging 30(5):781–793. doi:10.1007/s00259-003-1184-3
28. Gotthardt M, Fischer M, Naeher I, Holz JB, Jungclas H, Fritsch HW, Behe M, Goke B, Joseph K, Behr TM (2002) Use of the incretin hormone glucagon-like peptide-1 (GLP-1) for the detection of insulinomas: initial experimental results. Eur J Nucl Med Mol Imaging 29(5):597–606. doi:10.1007/s00259-002-0761-1
29. Brom M, Oyen WJ, Joosten L, Gotthardt M, Boerman OC (2010) 68 Ga-labelled exendin-3, a new agent for the detection of insulinomas with PET. Eur J Nucl Med Mol Imaging 37(7):1345–1355. doi:10.1007/s00259-009-1363-y
30. Wild D, Behe M, Wicki A, Storch D, Waser B, Gotthardt M, Keil B, Christofori G, Reubi JC, Macke HR (2006) [Lys^{40}(Ahx-DTPA-^{111}In)NH$_2$]Exendin-4, a very promising ligand

for glucagon-like peptide-1 (GLP-1) receptor targeting. J Nucl Med 47(12):2025–2033
31. Wild D, Macke H, Christ E, Gloor B, Reubi JC (2008) Glucagon-like peptide 1-receptor scans to localize occult insulinomas. N Engl J Med 359(7):766–768. doi:10.1056/NEJMc0802045
32. Wild D, Wicki A, Mansi R, Behe M, Keil B, Bernhardt P, Christofori G, Ell PJ, Macke HR (2010) Exendin-4-based radiopharmaceuticals for glucagon-like peptide-1 receptor PET/CT and SPECT/CT. J Nucl Med 51(7):1059–1067. doi:10.2967/jnumed.110.074914
33. Antwi K, Fani M, Nicolas G, Rottenburger C, Heye T, Reubi JC, Gloor B, Christ E, Wild D (2015) Localization of hidden insulinomas with ^{68}Ga-DOTA-exendin-4 PET/CT: a pilot study. J Nucl Med 56(7):1075–1078. doi:10.2967/jnumed.115.157768
34. Gao H, Niu G, Yang M, Quan Q, Ma Y, Murage EN, Ahn JM, Kiesewetter DO, Chen X (2011) PET of insulinoma using ^{18}F-FBEM-EM3106B, a new GLP-1 analogue. Mol Pharm 8(5):1775–1782. doi:10.1021/mp200141x
35. Kiesewetter DO, Gao H, Ma Y, Niu G, Quan Q, Guo N, Chen X (2012) ^{18}F-radiolabeled analogs of exendin-4 for PET imaging of GLP-1 in insulinoma. Eur J Nucl Med Mol Imaging 39(3):463–473. doi:10.1007/s00259-011-1980-0
36. Kiesewetter DO, Guo N, Guo J, Gao H, Zhu L, Ma Y, Niu G, Chen X (2012) Evaluation of an [^{18}F]AlF-NOTA analog of exendin-4 for imaging of GLP-1 receptor in insulinoma. Theranostics 2(10):999–1009. doi:10.7150/thno.5276
37. Wang Y, Lim K, Normandin M, Zhao X, Cline GW, Ding YS (2012) Synthesis and evaluation of [^{18}F]exendin (9-39) as a potential biomarker to measure pancreatic beta-cell mass. Nucl Med Biol 39(2):167–176. doi:10.1016/j.nucmedbio.2011.07.011
38. Wu Z, Liu S, Hassink M, Nair I, Park R, Li L, Todorov I, Fox JM, Li Z, Shively JE, Conti PS, Kandeel F (2013) Development and evaluation of ^{18}F-TTCO-Cys^{40}-Exendin-4: a PET probe for imaging transplanted islets. J Nucl Med 54(2):244–251. doi:10.2967/jnumed.112.109694
39. Wu Z, Todorov I, Li L, Bading JR, Li Z, Nair I, Ishiyama K, Colcher D, Conti PE, Fraser SE, Shively JE, Kandeel F (2011) In vivo imaging of transplanted islets with ^{64}Cu-DO3A-VS-Cys^{40}-Exendin-4 by targeting GLP-1 receptor. Bioconjug Chem 22(8):1587–1594. doi:10.1021/bc200132t
40. Wu Z, Liu S, Nair I, Omori K, Scott S, Todorov I, Shively JE, Conti PS, Li Z, Kandeel F (2014) ^{64}Cu labeled sarcophagine exendin-4 for microPET imaging of glucagon-like peptide-1 receptor expression. Theranostics 4(8):770–777. doi:10.7150/thno.7759
41. Connolly BM, Vanko A, McQuade P, Guenther I, Meng X, Rubins D, Waterhouse R, Hargreaves R, Sur C, Hostetler E (2012) Ex vivo imaging of pancreatic beta cells using a radiolabeled GLP-1 receptor agonist. Mol Imaging Biol 14(1):79–87. doi:10.1007/s11307-011-0481-7
42. Mikkola K, Yim CB, Fagerholm V, Ishizu T, Elomaa VV, Rajander J, Jurttila J, Saanijoki T, Tolvanen T, Tirri M, Gourni E, Behe M, Gotthardt M, Reubi JC, Macke H, Roivainen A, Solin O, Nuutila P (2014) 64Cu- and 68 Ga-labelled [Nle14, Lys40(Ahx-NODAGA) NH2]-exendin-4 for pancreatic beta cell imaging in rats. Mol Imaging Biol 16(2):255–263. doi:10.1007/s11307-013-0691-2
43. Selvaraju RK, Velikyan I, Johansson L, Wu Z, Todorov I, Shively J, Kandeel F, Korsgren O, Eriksson O (2013) In vivo imaging of the glucagon-like peptide 1 receptor in the pancreas with ^{68}Ga-labeled DO3A-exendin-4. J Nucl Med 54(8):1458–1463. doi:10.2967/jnumed.112.114066
44. Selvaraju RK, Velikyan I, Asplund V, Johansson L, Wu Z, Todorov I, Shively J, Kandeel F, Eriksson B, Korsgren O, Eriksson O (2014) Pre-clinical evaluation of [^{68}Ga]Ga-DO3A-VS-Cys^{40}-Exendin-4 for imaging of insulinoma. Nucl Med Biol 41(6):471–476. doi:10.1016/j.nucmedbio.2014.03.017
45. Nalin L, Selvaraju RK, Velikyan I, Berglund M, Andreasson S, Wikstrand A, Ryden A, Lubberink M, Kandeel F, Nyman G, Korsgren O, Eriksson O, Jensen-Waern M (2014) Positron emission tomography imaging of the glucagon-like peptide-1 receptor in healthy and streptozotocin-induced diabetic pigs. Eur J Nucl Med Mol Imaging 41(9):1800–1810. doi:10.1007/s00259-014-2745-3
46. Di Gialleonardo V, Signore A, Scheerstra EA, Visser AK, van Waarde A, Dierckx RA, de Vries EF (2012) ^{11}C-hydroxytryptophan uptake and metabolism in endocrine and exocrine pancreas. J Nucl Med 53(11):1755–1763. doi:10.2967/jnumed.112.104117
47. Eriksson O, Espes D, Selvaraju RK, Jansson E, Antoni G, Sörensen J, Lubberink M, Biglarnia A-R, Eriksson JW, Sundin A (2014) Positron emission tomography ligand [^{11}C] 5-hydroxytryptophan can be used as a surrogate marker for the human endocrine pancreas. Diabetes 63(10):3428–3437
48. Eriksson O, Velikyan I, Selvaraju RK, Kandeel F, Johansson L, Antoni G, Eriksson B, Sorensen J, Korsgren O (2014) Detection of metastatic insulinoma by positron emission tomography with [^{68}Ga]exendin-4-a case report. J Clin Endocrinol Metab 99(5):1519–1524. doi:10.1210/jc.2013-3541
49. Luo Y, Yu M, Pan Q, Wu W, Zhang T, Kiesewetter DO, Zhu Z, Li F, Chen X, Zhao Y (2015) ^{68}Ga-NOTA-exendin-4 PET/CT in detection of occult insulinoma and evaluation of physiological uptake. Eur J Nucl Med Mol Imaging 42(3):531–532. doi:10.1007/s00259-014-2946-9
50. Luo Y, Pan Q, Yao S, Yu M, Wu W, Xue H, Kiesewetter DO, Zhu Z, Li F, Zhao Y, Chen X (2016) Glucagon-like peptide-1 receptor PET/CT with ^{68}Ga-NOTA-Exendin-4 for detecting localized insulinoma: a prospective cohort study. J Nucl Med 57(5):715–720. doi:10.2967/jnumed.115.167445
51. Velikyan I, Selvaraju R, Bulenga T, Espes D, Lubberink M, Sörensen J, Eriksson B, Estrada S, Eriksson O (2015) Dosimetry of [^{68}Ga]Ga-DO3A-VS-Cys^{40}-Exendin-4 in rodents, pigs, non-human primates and human. J Labelled Comp Radiopharm 58(3):S95
52. Wimalasena K (2011) Vesicular monoamine transporters: structure-function, pharmacology, and medicinal chemistry. Med Res Rev 31(4):483–519. doi:10.1002/med.20187
53. Maffei A, Liu Z, Witkowski P, Moschella F, Del Pozzo G, Liu E, Herold K, Winchester RJ, Hardy MA, Harris PE (2004) Identification of tissue-restricted transcripts in human islets. Endocrinology 145(10):4513–4521. doi:10.1210/en.2004-0691
54. Anlauf M, Eissele R, Schafer MK, Eiden LE, Arnold R, Pauser U, Kloppel G, Weihe E (2003) Expression of the two isoforms of the vesicular monoamine transporter (VMAT1 and VMAT2) in the endocrine pancreas and pancreatic endocrine tumors. J Histochem Cytochem 51(8):1027–1040. doi:10.1177/002215540305100806
55. Ichise M, Harris PE (2010) Imaging of beta-cell mass and function. J Nucl Med 51(7):1001–1004. doi:10.2967/jnumed.109.068999
56. Souza F, Freeby M, Hultman K, Simpson N, Herron A, Witkowsky P, Liu E, Maffei A, Harris PE (2006) Current progress in non-invasive imaging of beta cell mass of the endocrine pancreas. Curr Med Chem 13(23):2761–2773. doi:10.2174/092986706778521940
57. Bohnen NI, Albin RL, Koeppe RA, Wernette KA, Kilbourn MR, Minoshima S, Frey KA (2006) Positron emission tomography of monoaminergic vesicular binding in aging and Parkinson disease. J Cereb Blood Flow Metab 26(9):1198–1212. doi:10.1038/sj.jcbfm.9600276
58. Erickson JD, Schafer MKH, Bonner TI, Eiden LE, Weihe E (1996) Distinct pharmacological properties and distribution in neurons and endocrine cells of two isoforms of the human vesicular monoamine transporter. Proc Natl Acad Sci USA 93(10):5166–5171. doi:10.1073/pnas.93.10.5166

59. DaSilva JN, Kilbourn MR, Mangner TJ (1993) Synthesis of [11C] tetrabenazine, a vesicular monoamine uptake inhibitor, for PET imaging studies. Appl Radiat Isot 44(4):673–676
60. Jewett DM, Kilbourn MR, Lee LC (1997) A simple synthesis of [^{11}C]dihydrotetrabenazine (DTBZ). Nucl Med Biol 24(2):197–199
61. DaSilva JN, Kilbourn MR, Mangner TJ (1993) Synthesis of a [^{11}C]methoxy derivative of alpha-dihydrotetrabenazine: a radioligand for studying the vesicular monoamine transporter. Appl Radiat Isot 44(12):1487–1489
62. DaSilva JN, Kilbourn MR (1992) In vivo binding of [^{11}C]tetrabenazine to vesicular monoamine transporters in mouse brain. Life Sci 51(8):593–600. doi:10.1016/0024-3205(92)90228-H
63. Dasilva JN, Carey JE, Sherman PS, Pisani TJ, Kilbourn MR (1994) Characterization of [^{11}C]tetrabenazine as an in vivo radioligand for the vesicular monoamine transporter. Nucl Med Biol 21(2):151–156. doi:10.1016/0969-8051(94)90003-5
64. Kilbourn M, Lee L, Vander BT, Jewett D, Frey K (1995) Binding of alpha-dihydrotetrabenazine to the vesicular monoamine transporter is stereospecific. Eur J Pharmacol 278(3):249–252
65. Simpson NR, Souza F, Witkowski P, Maffei A, Raffo A, Herron A, Kilbourn M, Jurewicz A, Herold K, Liu E, Hardy MA, Van Heertum R, Harris PE (2006) Visualizing pancreatic beta-cell mass with [^{11}C]DTBZ. Nucl Med Biol 33(7):855–864. doi:10.1016/j.nucmedbio.2006.07.002
66. Goland R, Freeby M, Parsey R, Saisho Y, Kumar D, Simpson N, Hirsch J, Prince M, Maffei A, Mann JJ, Butler PC, Van Heertum R, Leibel RL, Ichise M, Harris PE (2009) ^{11}C-dihydrotetrabenazine PET of the pancreas in subjects with long-standing type 1 diabetes and in healthy controls. J Nucl Med 50(3):382–389. doi:10.2967/jnumed.108.054866
67. Harris PE, Ferrara C, Barba P, Polito T, Freeby M, Maffei A (2008) VMAT2 gene expression and function as it applies to imaging beta-cell mass. J Mol Med (Berl) 86(1):5–16. doi:10.1007/s00109-007-0242-x
68. Kung HF, Lieberman BP, Zhuang ZP, Oya S, Kung MP, Choi SR, Poessl K, Blankemeyer E, Hou C, Skovronsky D, Kilbourn M (2008) In vivo imaging of vesicular monoamine transporter 2 in pancreas using an (18)F epoxide derivative of tetrabenazine. Nucl Med Biol 35(8):825–837. doi:10.1016/j.nucmedbio.2008.08.004
69. Kung M-P, Hou C, Lieberman BP, Oya S, Ponde DE, Blankemeyer E, Skovronsky D, Kilbourn MR, Kung HF (2008) In vivo imaging of β-cell mass in rats using ^{18}F-FP-(+)-DTBZ: a potential PET ligand for studying diabetes mellitus. J Nucl Med 49(7):1171–1176
70. Normandin MD, Petersen KF, Ding YS, Lin SF, Naik S, Fowles K, Skovronsky DM, Herold KC, McCarthy TJ, Calle RA, Carson RE, Treadway JL, Cline GW (2012) In vivo imaging of endogenous pancreatic beta-cell mass in healthy and type 1 diabetic subjects using ^{18}F-fluoropropyl-dihydrotetrabenazine and PET. J Nucl Med 53(6):908–916. doi:10.2967/jnumed.111.100545
71. Singhal T, Ding YS, Weinzimmer D, Normandin MD, Labaree D, Ropchan J, Nabulsi N, Lin SF, Skaddan MB, Soeller WC, Huang Y, Carson RE, Treadway JL, Cline GW (2011) Pancreatic beta cell mass PET imaging and quantification with [^{11}C]DTBZ and [^{18}F]FP-(+)-DTBZ in rodent models of diabetes. Mol Imaging Biol 13(5):973–984. doi:10.1007/s11307-010-0406-x
72. Tsao HH, Skovronsky DM, Lin KJ, Yen TC, Wey SP, Kung MP (2011) Sigma receptor binding of tetrabenazine series tracers targeting VMAT2 in rat pancreas. Nucl Med Biol 38(7):1029–1034. doi:10.1016/j.nucmedbio.2011.03.006
73. Harris PE, Farwell MD, Ichise M (2013) PET quantification of pancreatic VMAT 2 binding using (+) and (−) enantiomers of [^{18}F]FP-DTBZ in baboons. Nucl Med Biol 40(1):60–64. doi:10.1016/j.nucmedbio.2012.09.003
74. Eriksson O, Jahan M, Johnstrom P, Korsgren O, Sundin A, Halldin C, Johansson L (2010) In vivo and in vitro characterization of [^{18}F]-FE-(+)-DTBZ as a tracer for beta-cell mass. Nucl Med Biol 37(3):357–363. doi:10.1016/j.nucmedbio.2009.12.004
75. Zhang M-R, Tsuchiyama A, Haradahira T, Yoshida Y, Furutsuka K, Suzuki K (2002) Development of an automated system for synthesizing ^{18}F-labeled compounds using [^{18}F]fluoroethyl bromide as a synthetic precursor. Appl Radiat Isot 57(3):335–342. doi:10.1016/s0969-8043(02)00075-1
76. Jahan M, Eriksson O, Johnstrom P, Korsgren O, Sundin A, Johansson L, Halldin C (2011) Decreased defluorination using the novel beta-cell imaging agent [^{18}F]FE-DTBZ-d4 in pigs examined by PET. EJNMMI Res 1(1):33. doi:10.1186/2191-219X-1-33
77. Kumar A, Lo ST, Oz OK, Sun X (2014) Derivatization of (+/−) dihydrotetrabenazine for copper-64 labeling towards long-lived radiotracers for PET imaging of the vesicular monoamine transporter 2. Bioorg Med Chem Lett 24(24):5663–5665. doi:10.1016/j.bmcl.2014.10.070
78. Lindskog C, Korsgren O, Ponten F, Eriksson JW, Johansson L, Danielsson A (2012) Novel pancreatic beta cell-specific proteins: antibody-based proteomics for identification of new biomarker candidates. J Proteomics 75(9):2611–2620. doi:10.1016/j.jprot.2012.03.008
79. Hellstrom-Lindahl E, Danielsson A, Ponten F, Czernichow P, Korsgren O, Johansson L, Eriksson O (2016) GPR44 is a pancreatic protein restricted to the human beta cell. Acta Diabetol 53(3):413–421. doi:10.1007/s00592-015-0811-3
80. Jahan M (2016) Mahabuba Jahan. Development of novel PET radioligands for visualizing beta cell mass and amyloid plaques. PhD thesis
81. Roep BO, Peakman M (2012) Antigen targets of type 1 diabetes autoimmunity. Cold Spring Harb Perspect Med 2(4):a007781. doi:10.1101/cshperspect.a007781
82. Moore A, Bonner-Weir S, Weissleder R (2001) Noninvasive in vivo measurement of beta-cell mass in mouse model of diabetes. Diabetes 50(10):2231–2236. doi:10.2337/diabetes.50.10.2231
83. Ladriere L, Malaisse-Lagae F, Alejandro R, Malaisse WJ (2001) Pancreatic fate of a ^{125}I-labelled mouse monoclonal antibody directed against pancreatic B-cell surface ganglioside(s) in control and diabetic rats. Cell Biochem Funct 19(2):107–115. doi:10.1002/cbf.903
84. Jahan M, Johnstrom P, Nag S, Takano A, Korsgren O, Johansson L, Halldin C, Eriksson O (2015) Synthesis and biological evaluation of [^{11}C]AZ12504948; a novel tracer for imaging of glucokinase in pancreas and liver. Nucl Med Biol 42(4):387–394. doi:10.1016/j.nucmedbio.2014.12.003
85. Min JJ, Gambhir SS (2008) Molecular imaging of PET reporter gene expression. Handb Exp Pharmacol 185(185 Pt 2):277–303. doi:10.1007/978-3-540-77496-9_12
86. Tai JH, Nguyen B, Wells RG, Kovacs MS, McGirr R, Prato FS, Morgan TG, Dhanvantari S (2008) Imaging of gene expression in live pancreatic islet cell lines using dual-isotope SPECT. J Nucl Med 49(1):94–102. doi:10.2967/jnumed.107.043430
87. Kim SJ, Doudet DJ, Studenov AR, Nian C, Ruth TJ, Gambhir SS, McIntosh CH (2006) Quantitative micro positron emission tomography (PET) imaging for the in vivo determination of pancreatic islet graft survival. Nat Med 12(12):1423–1428. doi:10.1038/nm1458
88. Lu Y, Dang H, Middleton B, Zhang Z, Washburn L, Stout DB, Campbell-Thompson M, Atkinson MA, Phelps M, Gambhir SS, Tian J, Kaufman DL (2006) Noninvasive imaging of islet grafts using positron-emission tomography. Proc Natl Acad Sci USA 103(30):11294–11299. doi:10.1073/pnas.0603909103
89. McGirr R, Hu S, Yee SP, Kovacs MS, Lee TY, Dhanvantari S (2011) Towards PET imaging of intact pancreatic beta cell mass: a transgenic strategy. Mol Imaging Biol 13(5):962–972. doi:10.1007/s11307-010-0435-5

90. Shapiro AJ, Hao EG, Lakey JR, Yakimets WJ, Churchill TA, Mitlianga PG, Papadopoulos GK, Elliott JF, Rajotte RV, Kneteman NM (2001) Novel approaches toward early diagnosis of islet allograft rejection. Transplantation 71(12):1709–1718
91. Shapiro AMJ, Lakey JRT, Ryan EA, Korbutt GS, Toth E, Warnock GL, Kneteman NM, Rajotte RV (2000) Islet transplantation in seven patients with type 1 diabetes mellitus using a glucocorticoid-free immunosuppressive regimen. N Engl J Med 343(4):230–238. doi:10.1056/Nejm200007273430401
92. Sowa-Staszczak A, Pach D, Mikołajczak R, Mäcke H, Jabrocka-Hybel A, Stefańska A, Tomaszuk M, Janota B, Gilis-Januszewska A, Małecki M (2013) Glucagon-like peptide-1 receptor imaging with [Lys^{40}(Ahx-HYNIC-^{99m}Tc/EDDA) NH_2]-exendin-4 for the detection of insulinoma. EurJ Nucl Med Mol Imaging 40(4):524–531
93. Martin WH, Delbeke D, Patton JA, Sandler MP (1996) Detection of malignancies with SPECT versus PET, with 2-[fluorine-18]fluoro-2-deoxy-D-glucose. Radiology 198(1):225–231. doi:10.1148/radiology.198.1.8539384
94. Brom M, Woliner-Van Der Weg W, Joosten L, Frielink C, Bouckenooghe T, Rijken P, Andralojc K, Göke BJ, de Jong M, Eizirik DL (2014) Non-invasive quantification of the beta cell mass by SPECT with ^{111}In-labelled exendin. Diabetologia 57(5):950–959
95. Rahier J, Goebbels RM, Henquin JC (1983) Cellular composition of the human diabetic pancreas. Diabetologia 24(5):366–371
96. Herrera PL (2003) Defining the cell lineages of the islets of Langerhans using transgenic mice. Int J Dev Biol 46(1):97–103
97. Fagerholm V, Mikkola KK, Ishizu T, Arponen E, Kauhanen S, Nagren K, Solin O, Nuutila P, Haaparanta M (2010) Assessment of islet specificity of dihydrotetrabenazine radiotracer binding in rat pancreas and human pancreas. J Nucl Med 51(9):1439–1446. doi:10.2967/jnumed.109.074492
98. Hellström-Lindahl E, Danielsson A, Ponten F, Czernichow P, Korsgren O, Johansson L, Eriksson O (2016) GPR44 is a pancreatic protein restricted to the human beta cell. Acta Diabetol 53(3):413–421